

The 3.3 μm PAH emission band of the Red Rectangle

In-Ok Song^{1,2}, J. McCombie¹, T. H. Kerr³ and P. J. Sarre¹

¹*School of Chemistry, The University of Nottingham, University Park, Nottingham NG7 2RD, U.K.*

²*Department of Astronomy and Space Science, Kyung Hee University, Suwon, 446-701, Korea.*

³*United Kingdom Infrared Telescope, Joint Astronomy Centre, 660 N. A'ohoku Place, University Park, Hilo, Hawaii 96720, U.S.A.*

Accepted. Received.

ABSTRACT

A new analysis of long-slit CGS4 (UKIRT) spectra of the 3.3 μm feature of the Red Rectangle and its evolution with offset along the NW whisker of the nebula is presented. The results support a proposed two-component interpretation for the 3.3 μm feature with peak wavelengths near 3.28 μm and 3.30 μm . Both components exhibit a small shift to shorter wavelength with increasing offset from the central star which, by comparison with laboratory studies, is consistent with a decrease in temperature of the carriers with distance from HD 44179. The two-component approach is also applied to 3.3 μm data for the Red Rectangle, Orion Bar D2 and Orion Bar H2S1 from ISO SWS studies.

Key words: stars: individual (Red Rectangle) – techniques: spectroscopic– ISM: molecules – ISM: lines and bands – ISM: abundances

1 INTRODUCTION

The unidentified infrared (UIR) bands are a family of emission features at 3.3, 6.2, 7.7, 8.6, 11.2 and 12.7 μm which are accompanied by several minor ones between 3 and 20 μm . They are believed to be due to C-H and C-C vibrational transitions of polycyclic aromatic hydrocarbon (PAH) molecules or small particles and have been observed in planetary and reflection nebulae, H II regions, young stellar objects, the general interstellar medium and galaxies such as ultraluminous infrared galaxies, star forming galaxies and active galactic nuclei.

Given the ubiquity of the bands in both Galactic sources and external galaxies and their widespread use as a probe of astronomical environments, improvement in understanding their origin is a high priority. For recent discussion of the UIR bands see Tokunaga (1997); Tielens et al. (1999); Van Kerckhoven et al. (2000); Sellgren (2001); Hony et al. (2001); Peeters et al. (2002a); van Diedenhoven et al. (2004). Considerable observational, theoretical and laboratory effort is being committed to PAH research and to the chemistry and physics of disks and nebular material of objects such as the Red Rectangle, particularly as this holds the prospect of providing much insight into the rôle of large molecules and dust in astronomy in general. It is notable that apart from the related monocyclic benzene molecule to which a narrow absorption line at 14.84 μm in CRL 618 has been assigned (Cernicharo et al. 2001) and blue fluorescence attributed to small PAHs in the Red Rectangle (Vijh, Witt & Gordon 2004, 2005a), there is no spectroscopic identification of an individual PAH in any astronomical environment.

The 3.3 μm feature is the shortest wavelength member of the UIR band family and is normally attributed to the C-H in-plane stretch vibration of PAHs. Most researchers consider that it arises from a superposition of infrared transitions of a number of gas-phase PAH species following absorption of ultraviolet/visible photons, although this is not the only proposed form of PAH material or proposed excitation mechanism. Its profile has been explored in various objects (Tokunaga et al. 1991; van Diedenhoven et al. 2004) and in some studies it is spatially resolved (Sloan et al. 1997; Geballe et al. 1989; Sellgren, Tokunaga & Nakada 1990; Kerr et al. 1999; Song et al. 2003; Geers et al. 2005). These studies have suggested that there is no link between the local radiation field and the profile of the 3.3 μm feature, but rather that the variation observed arises from compositional changes related to the age of the emitting material (Sellgren, Tokunaga & Nakada 1990; van Diedenhoven et al. 2004). However, a clear picture for the material composition has not yet emerged and a coherent model remains to be established.

Of all currently studied Galactic objects the Red Rectangle is one of the most fascinating for UIR band studies. It has a wealth of unidentified or partially identified emission features which fall in a wide spectral range from the near-IR to the far-UV (Cohen et al. 1975). It is a particularly attractive target because of the strength of the UIR bands and its well-defined biconical geometry that extends at least 40'' from the centre of the nebula (Cohen et al. 2004). A new 3.28 μm sub-feature was suggested by Song et al. (2003) in order to interpret the 3.3 μm band profile in the Red Rectangle.

In this paper we review briefly previous spectroscopic and imaging studies of the 3.3 μm emission feature (section 2), summarize observational aspects (section 3), and present a two-component analysis of long-slit CGS4 3.3 μm data for the Red Rectangle in section 4 with application also to ISO SWS 3.3 μm profiles of the Orion Bar (section 5). Discussion and summary/conclusions are given in sections 6 and 7, respectively.

2 THE C-H EMISSION FEATURE: A BRIEF REVIEW OF OBSERVATIONS

2.1 Spectroscopy and profile of the 3.3 μm band

The origin and nature of the 3.3 μm band has been discussed by a number of authors (Sellgren, Tokunaga & Nakada 1990; Tokunaga et al. 1991; van Diedenhoven et al. 2004). The profile is known to vary between and within objects and an (**A**, **B**) classification has been put forward by van Diedenhoven et al. (2004) with particular reference to ISO SWS data. The **A**_{3.3} group is common and has a profile described as ‘symmetric’ with peak position at $\sim 3.290 \mu\text{m}$ and a FWHM of 0.040 μm . This profile is found in widely differing objects ranging from Orion Bar H2S1 to NGC 7027 and is similar to Type 1 ($\lambda_{max} \sim 3.289 \mu\text{m}$; FWHM $\leq 0.042 \mu\text{m}$) in the earlier classification of Tokunaga et al. (1991). Group **B**_{1.3.3} with maximum at $\sim 3.293 \mu\text{m}$ (FWHM $\sim 0.037 \mu\text{m}$) and group **B**_{2.3.3} with a peak wavelength at $\sim 3.297 \mu\text{m}$ (FWHM $\sim 0.037 \mu\text{m}$) are found in relatively few objects, an example of **B**_{1.3.3} being Orion Bar D2.

The overall Red Rectangle spectrum is classified as **B**_{2.3.3} where this comprises a $14'' \times 20''$ exposure of both star and nebula. The 3.3 μm profile directly on the star HD 44179 is fitted very well by a single Lorentzian function (Song et al. 2003); it is of the rarer Type 2 in the Tokunaga et al. (1991) description. Hence the ISO SWS (**B**_{2.3.3}) Red Rectangle spectrum is a superposition of Type 2 and 1 where the latter persists in the nebula. Song et al. (2003) showed that the development of a short-wavelength shoulder on the 3.3 μm feature with increasing offset from the central star could be interpreted in terms of the growth of a new band with a peak wavelength of 3.28 μm . This represents the evolution from a Type 2 to Type 1 (**A**_{3.3}) profile.

We describe in this paper a refined analysis of the spatially resolved Red Rectangle data of Song et al. (2003) which supports the existence of the proposed 3.28 μm band and establishes small blueward shifts in peak wavelength with offset for both components of the overall 3.3 μm feature. The same approach is applied to some ISO SWS targets in section 5. We use the nominal description ‘3.3’ μm to refer to the whole 3.3 μm profile irrespective of shape, with the wavelengths of the components written with a second decimal place *viz* 3.28 μm and 3.30 μm .

2.2 Imaging and spatially-resolved studies

The binary star (Waelkens et al. 1996) of the Red Rectangle is obscured by a disk that lies close to the W-E axis (Roddier et al. 1995; Osterbart, Langer & Weigelt 1997; Tuthill et al. 2002; Waters et al. 1998). The *inner*

region of $\leq 1''$ has been the subject of high-spatial-resolution imaging infrared studies (Roddier et al. 1995; Osterbart, Langer & Weigelt 1997; Men’shchikov et al. 1998, 2002; Mékarnia et al. 1998; Tuthill et al. 2002; Murakawa et al. 2003; Miyata et al. 2004) and radio mapping in CO (Bujarrabal et al. 2005). In the study of Song et al. (2003) the slit was positioned (a) directly on HD 44179 and (b) aligned along the NW interface but offset by $2''$ from the star.

The spatial distribution of IR emission in both the 3.3 μm emission feature and the continuum for a *wider* region of the nebula has been investigated using both imaging and long-slit spectroscopic techniques. Bregman et al. (1993a) found the continuum-subtracted 3.3 μm distribution to be centrally peaked on the star and slightly extended N-S over a region up to *c.* $4''$ from the source at a spatial resolution of $\sim 0.5-1''$. At a higher spatial resolution of $\sim 0.2''$, Mékarnia et al. (1998) reported more detail in the 3.3 μm distribution and found elongation along the cone walls within $1-1.5''$ of the star about the N-S axis. Spectroscopic measurements by Kerr et al. (1999) with a slit in four positions placed $5''$ N, S, E and W of the star revealed 3.3 μm PAH emission nearly symmetrically distributed around the star at these higher offsets. Significantly there was no enhancement of 3.3 μm emission at the intersections of the slit with the bicone interfaces where the unidentified optical emission features peak in intensity.

The distribution of the 3.3 μm feature contrasts sharply with images taken in other C-H mode UIR bands. Bregman et al. (1993a) found that the 11.3 μm image shows a N-S bipolar shape with no central peak. Similar images have been reported by Hora et al. (1996) for a $5'' \times 5''$ region at the C-H-related UIR wavelengths of 8.6, 11.2 and 12.7 μm , but not for the continuum wavelengths of 10.0 and 20.2 μm which are centrally peaked. From these results it would appear that although the 3.3 μm feature is a PAH transition, it does not originate in the same class of PAHs that give rise to the C-H UIR bands at longer wavelengths. A spatial distinction between 3.3 μm and other PAH modes has also been found in NGC 1333 and the Orion bar and attributed to differences in the size of the carriers, with the 3.3 μm band arising in smaller PAHs (Bregman et al. 1993b, 1994).

3 OBSERVATIONAL DETAILS

3.1 UKIRT CGS4 observations of the Red Rectangle

The technical details and a log of the near-IR long-slit observations have been presented by Song et al. (2003). As this paper describes a new analysis of these data, we summarize here that they were recorded using the 1-5 μm CGS4 spectrometer with a 1-pixel wide slit ($0.6''$) and a 256×256 InSb array giving a resolving power of 1000 at 3.3 μm . Spectra were taken with the $90''$ long slit aligned along the NW ‘whisker’. Except for recording an on-star spectrum, the slit was offset from the central star by $2''$ in order to avoid saturation of the CCD by the flux of the star.

Table 1. Intensity, peak wavelength and FWHM of the overall 3.3 μm band as a function of offset from HD 44179 along the NW interface of the nebula. Columns 3 and 4 are the values obtained from the best (single) Lorentzian fit to the asymmetric profile (see text).

Offset/ arcsec	Intensity/ 10^{-25}Wcm^{-2}	Peak Wavelength/ μm (cm^{-1})	FWHM/ μm (cm^{-1})
2.00	379.58	3.297 (3033)	0.036 (33)
2.61	266.89	3.297 (3033)	0.035 (32)
3.22	60.54	3.297 (3033)	0.034 (31)
3.83	11.01	3.295 (3035)	0.034 (32)
4.44	4.01	3.293 (3036)	0.036 (33)
5.05	2.02	3.293 (3037)	0.037 (34)
5.66	1.17	3.293 (3037)	0.038 (35)
6.27	0.72	3.292 (3037)	0.039 (36)
6.88	0.51	3.291 (3038)	0.040 (37)
7.49	0.38	3.291 (3038)	0.041 (38)
8.10	0.27	3.292 (3038)	0.041 (37)
8.71	0.19	3.291 (3039)	0.042 (39)
9.32	0.14	3.290 (3040)	0.043 (40)
9.93	0.13	3.290 (3040)	0.050 (46)
10.54	0.10	3.290 (3039)	0.045 (42)

3.2 ISO SWS observations

ISO data for these objects were taken from van Dienenhoven et al. (2004) and used in their published form. The spectra were obtained with the SWS (de Graauw et al. 1996) with a resolving power of 500-1500, processed using the package IA3, and rebinned with a constant resolution as described in Peeters et al. (2002b).

4 RED RECTANGLE AND ISO SWS SPECTRA

4.1 Two-component analysis of the 3.3 μm profile of the Red Rectangle

The overall 3.3 μm band maximum shifts to shorter wavelength, increases in width and declines rapidly in intensity with offset from HD 44179 along the NW interface. This is summarized in table 1 where a single Lorentzian fit to the 3.3 μm band was employed to illustrate these characteristics. However, the band shape in the nebula is *asymmetric* and varies as shown for offsets between 2'' and 10'' in figures 1 and 2. Song et al. (2003) suggested that the evolution of the profile could be interpreted in terms of the emergence of a new 3.28 μm band which gave the overall appearance of a shoulder on the short-wavelength side. There is no evidence for a 3.28 μm component in the on-star spectrum which is symmetrical and very well fitted by a single Lorentzian with peak maximum at 3.298 μm and $\text{FWHM} = 32 \text{ cm}^{-1}$ ($\sim 0.035 \mu\text{m}$) as shown in fig 1. of Song et al. (2003). The 3.3 μm band in the nebula was previously analysed simply by taking the fit to the on-star spectrum and subtracting this from the recorded profiles at the various distances into the nebula. Here we employ an improved approach in which the overall 3.3 μm band is fitted with two Lorentzians, allowing the intensities, peak wavelengths and widths to float in the fitting procedure (`splot` in IRAF – which uses the Levenberg-Marquardt optimisation). The results of the new fitting for offsets between 2'' and 8'' along the NW axis are

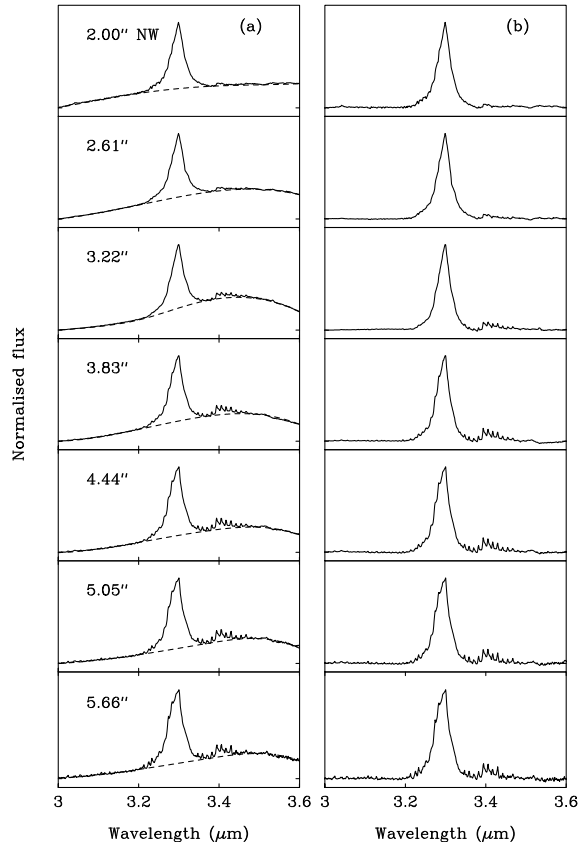


Figure 1. Spatially resolved spectra (solid line) of the 3.3 μm feature 2-6'' along the NW interface of the Red Rectangle with (a) a polynomial fit to the continuum (dashed line), and (b) continuum-subtracted spectra.

shown in fig. 3 where the importance of the 3.28 μm contribution is seen to grow with offset. The 3.28 $\mu\text{m}/3.30 \mu\text{m}$ ratio grows approximately linearly with distance as shown in fig. 4 and suggests that at very high offset (towards the ISM) the 3.28 μm feature would dominate. This is consistent with the observation of a 3.28 μm absorption feature towards the Galactic centre (Chiar et al. 2000; Song et al. 2003). We consider possible origins of the 3.30 and 3.28 μm components in the next section.

The peak maxima of the two components from the fit shift to slightly shorter wavelength with distance from HD 44179 (see fig. 5). The blueward shifts of the peak wavelength between 2'' and 8'' are $\sim 2 \text{ cm}^{-1}$ and $\sim 4 \text{ cm}^{-1}$ for the 3.30 and 3.28 μm components, respectively (fig. 5). The widths of the components appear to show some variation with offset (see fig. 6) and, if confirmed, may be due to changes in the PAH size distribution with offset. If the shift is caused by a reduction in internal temperature of the carriers and if the carriers are indeed gas-phase molecules, the direction of the shift is in the sense expected in comparison with experimental and theoretical data for gas-phase PAHs (Joblin et al. 1995). Laboratory studies of the 3.3 μm *absorption* bands of naphthalene (C_{10}H_8), pyrene ($\text{C}_{16}\text{H}_{10}$), coronene ($\text{C}_{24}\text{H}_{12}$) and ovalene ($\text{C}_{32}\text{H}_{14}$) as a function of temperature show that the temperature-

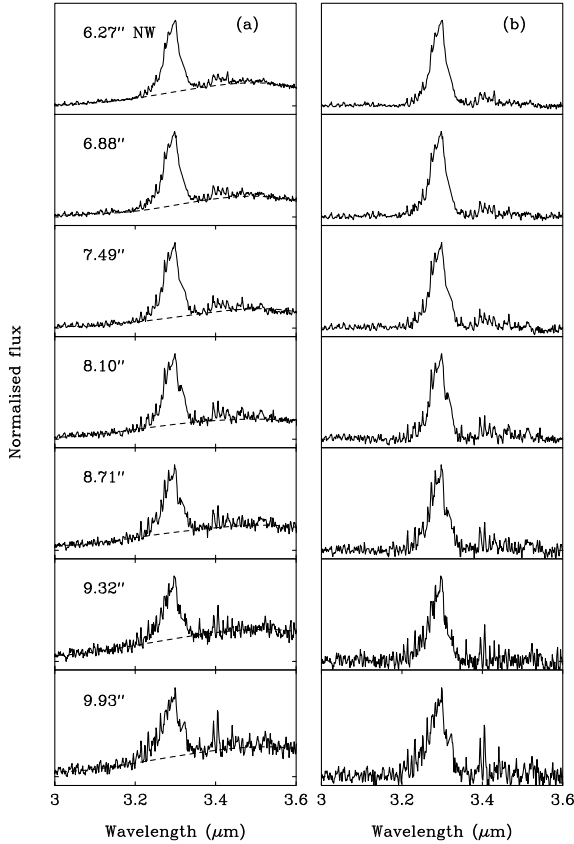


Figure 2. Spatially resolved spectra (solid line) of the $3.3\ \mu\text{m}$ feature $6\text{--}10''$ along the NW interface of the Red Rectangle with (a) a polynomial fit to the continuum (dashed line), and (b) continuum-subtracted spectra.

dependent frequency shift for these molecules increases with molecular size with values of $c. -0.0139, -0.0284, -0.0328$ and $-0.042\ \text{cm}^{-1}\text{K}^{-1}$, respectively (Joblin et al. 1995). The largest of these laboratory coefficients suggests a carrier temperature reduction of only $\sim 100\ \text{K}$ over $2\text{--}8''$. However, given that the infrared emission is thought to arise from rapid heating due to photon absorption rather than through thermal emission, this small temperature reduction is probably acceptable. The lower frequency shift with offset for the $3.30\ \mu\text{m}$ component (the one most prominent on-star) suggests that this feature arises in smaller PAHs than those that give rise to the $3.28\ \mu\text{m}$ band which is (relatively) stronger in the nebula. The temperature dependence of the width of the laboratory $3.3\ \mu\text{m}$ absorption feature on molecular size is less pronounced ranging from $0.0353\ \text{cm}^{-1}\text{K}^{-1}$ for naphthalene to $0.056\ \text{cm}^{-1}\text{K}^{-1}$ for ovalene (Joblin et al. 1995). This is qualitatively consistent with the astrophysical observations.

4.2 Origin of two $3.3\ \mu\text{m}$ components

Possible interpretations for the existence of two components are that these arise from different structural forms, sizes or hydrogenation/ionisation states of the ensemble of UIR band emitters. Laboratory gas-phase *absorption* spectra

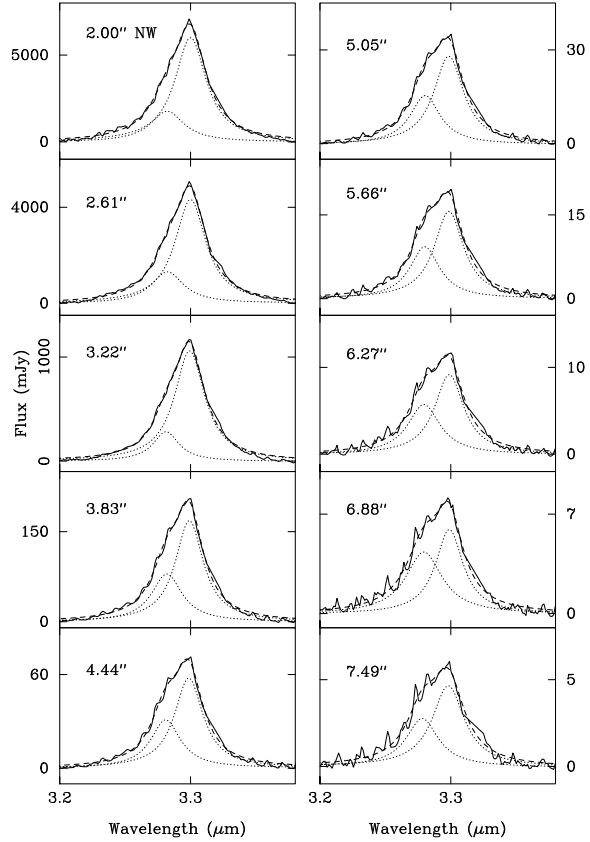


Figure 3. Fitted Lorentzian profiles as a function of offset from the central star. The solid lines are the observed spectra, the dotted lines are individual Lorentzian profiles and the dashed lines are the sum of the two profiles. The $3.28\ \mu\text{m}/3.30\ \mu\text{m}$ intensity ratio increases with offset.

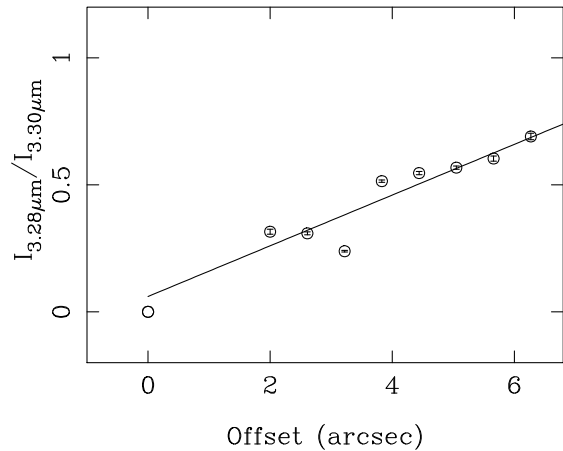


Figure 4. Plot of the $3.28\ \mu\text{m}/3.30\ \mu\text{m}$ intensity ratio as a function of offset from HD 44179 along the NW whisker of the Red Rectangle. The line is the result of an unweighted linear least-squares fit to the data above $2''$. There are no data points between 0 and $2''$ because the slit was offset from the star.

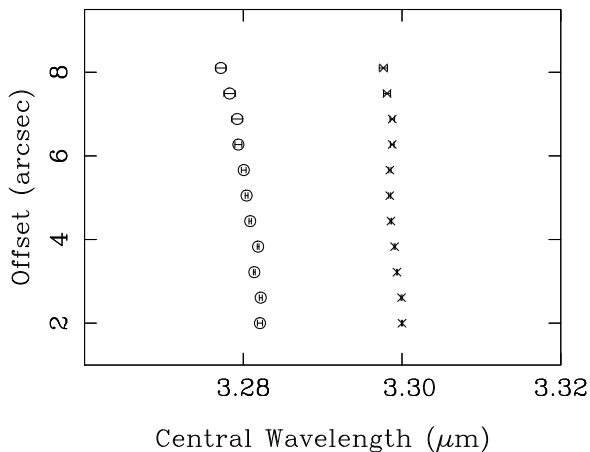


Figure 5. Plot of the central wavelength of the 3.28 (o) and 3.30 μm (x) components as a function of offset in the Red Rectangle. The values were obtained by Lorentzian fitting of the overall 3.3 μm profile (see text).

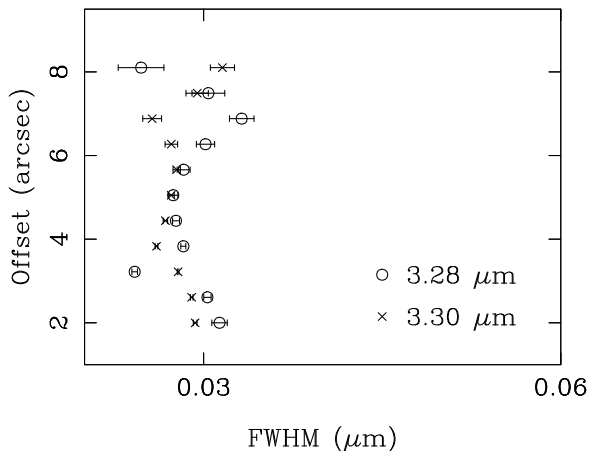


Figure 6. Plot of the width of the 3.28 (o) and 3.30 μm (x) components as a function of offset in the Red Rectangle. The values were obtained by Lorentzian fitting of the overall 3.3 μm profile (see text).

taken at elevated temperatures indicate that a blueward shift of the 3.3 μm peak maximum occurs with increasing PAH size of $c. 15 \text{ cm}^{-1}$ ($0.015 \mu\text{m}$) from pyrene ($\text{C}_{16}\text{H}_{10}$) to ovalene ($\text{C}_{32}\text{H}_{14}$) (Joblin et al. 1995). This is of the same magnitude as the $c. 0.02 \mu\text{m}$ difference between the 3.30 μm and 3.28 μm features discussed here. A wider range of gas-phase data particularly for larger PAHs would be of much interest. van Dienenhoven et al. (2004) comment that the 3.3 μm feature is attributable to the smallest emitting PAHs (Allamandola, Tielens & Barker 1989; Schutte, Tielens & Allamandola 1993), and report that within the NASA Ames laboratory sample of neutral PAH spectra taken in an inert gas matrix the C-H stretch frequency distribution is *bimodal* with the bands of the smallest PAHs centred near 3060 cm^{-1} (3.27 μm) and

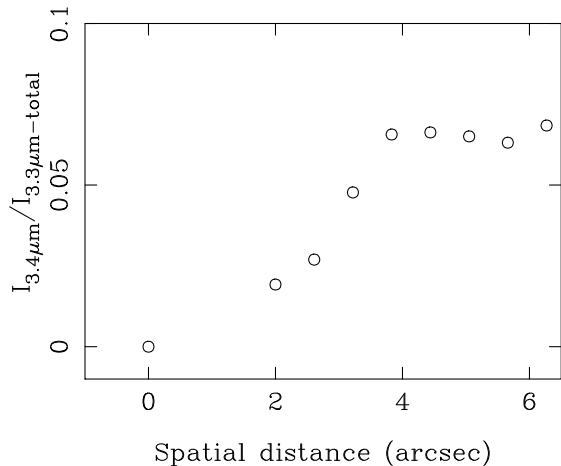


Figure 7. 3.4 μm /3.3 μm (integrated) intensity ratio along the NW whisker of the Red Rectangle. Residual telluric contamination in the 3.4 μm region makes it difficult to estimate the errors in this case.

transitions of larger PAHs occurring near $\sim 3090 \text{ cm}^{-1}$ (3.24 μm). The origin of this bimodal distribution is not clear. Applying a redward shift of $\sim 0.03 \mu\text{m}$ to these laboratory data, as is commonly invoked on account of the higher carrier temperature in the nebula (van Dienenhoven et al. 2004), yields wavelengths of 3.30 μm ($N_C \leq 40$) and 3.27 μm ($N_C \geq 40$) where N_C is the number of carbon atoms. These values are in good agreement with the wavelengths of the two components deduced in the analysis of Song et al. (2003) and considered further here. Finally we note that although laboratory data show that the 3.3 μm stretch frequency varies with PAH size and temperature, reported DFT B3LYP/4-31G C-H stretching frequencies are virtually independent of size being 3064, 3064 and 3062 cm^{-1} for $\text{C}_{24}\text{H}_{12}$ (coronene), $\text{C}_{54}\text{H}_{18}$ (circumcoronene) and $\text{C}_{96}\text{H}_{24}$ (Bauschlicher 2002).

4.3 Comparison of 3.4 μm and 3.28 μm emission of the Red Rectangle

As for the 3.28 μm band, the 3.4 μm emission is not present on-star but grows in strength relative to the 3.3 μm band with offset. This emission almost certainly arises from C-H motion of side groups such as $-\text{CH}_2$ and $-\text{CH}_3$ or from doubly hydrogenated sites (Geballe et al. 1989; Wagner, Kim & Saykally 2000; Pauzat & Ellinger 2001). Figure 7. shows a plot of the 3.4 μm /3.3 μm band ratio as a function of offset where the values run from zero on-star to ~ 0.06 at 4-6''; the trend may be compared with that for the 3.28 μm feature (figure 4). This (relative) growth in strength of the 3.4 μm band with offset is in the same sense as that found by Geballe et al. (1989) who, using a 5'' aperture, determined a 3.4 μm /3.3 μm ratio of 0.06 on-star (which includes part of the nebula) and 0.13 at a position 5'' N. It is striking that the 3.28 μm and 3.4 μm bands exhibit a very similar behaviour with increasing offset.

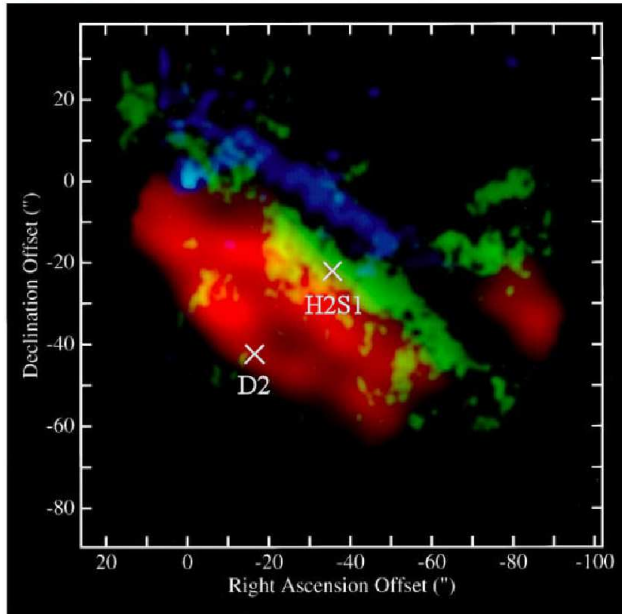


Figure 8. Orion Bar PDR showing the distribution of 3.3 μm PAH emission (blue), 2.12 μm H_2 $v=1-0$ S(1) emission (green) and ^{12}CO $J = 1-0$ emission (red). The star $\theta^2\text{A Ori}$ is at the (0,0) position at R.A. = 05 35 22.5, Dec. = -05 24 57.8 (2000). Reproduced (and adapted) with permission from Tielens et al. (1993)

5 APPLICATION OF TWO-COMPONENT ANALYSIS TO ISO SWS 3.3 μM SPECTRA

We have also applied the two-component fitting approach to 3.3 μm ISO data from van Dienenhoven et al. (2004) for Orion Bar H2S1 and D2 (see figure 8), and for the Red Rectangle ($14'' \times 20''$ *i.e.* central star plus nebula). The ISO 3.3 μm spectra for these objects together with the long-slit data for the Red Rectangle (on-star and 3.8'' offset) are shown in figure 9. Not only does the extent of the blue shoulder vary between objects, but the long-wavelength side of the feature also shifts slightly.

The results of two-component fitting of the Orion Bar D2 and Orion Bar H2S1 data are shown in figures 10 and 11 and may be compared with the spatially resolved fits for the Red Rectangle in figure 3. The spectral shape for Orion Bar D2 approximates to the higher offset region of the Red Rectangle, whereas the Orion Bar H2S1 profile is broader and symmetric (Class $\text{A}_{3.3}$).

Figure 12. presents the 3.28 $\mu\text{m}/3.30 \mu\text{m}$ integrated intensity ratios obtained from Lorentzian fitting. It includes the long-slit CGS4 3.3 μm ‘on-star’ data (\bullet) and shows the behaviour of the 3.28 $\mu\text{m}/3.30 \mu\text{m}$ ratio with increasing offset into the Red Rectangle nebula. The on-star profile is unique within this data set with no 3.28 μm component as noted previously (Song et al. 2003), so the ratio (y axis value in figure 12) is zero. From this analysis Orion Bar H2S1 has the highest 3.28 $\mu\text{m}/3.30 \mu\text{m}$ ratio and exceeds unity, with Orion Bar D2 and RR ISO data falling close to that for the $\sim 8''$ offset position of the Red Rectangle from the spatially-resolved CGS4 long-slit observations.

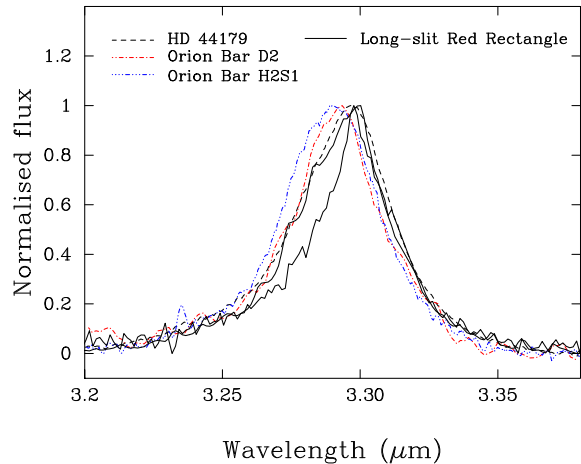


Figure 9. Normalised 3.3 μm profiles for three ISO SWS targets and long-slit Red Rectangle data (on-star and 3.8'' offset). The continuous lines represent the long-slit CGS4 Red Rectangle data, the inner trace being the on-star spectrum.

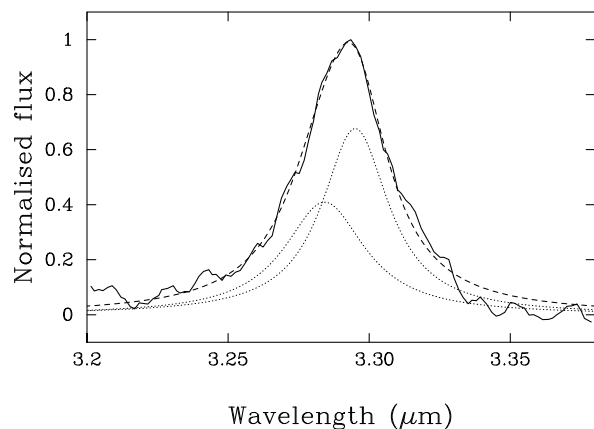


Figure 10. Two-component Lorentzian fit to the 3.3 μm profile towards Orion Bar D2 as recorded with ISO SWS.

6 DISCUSSION

We suggest that the variation in profile of the 3.3 μm PAH band is most readily interpreted in terms of the size distribution of neutral PAHs. The HD 44179 (on-star) 3.30 μm band is then characteristic of the smallest PAHs, with a larger PAH (3.28 μm) population growing with offset in the Red Rectangle in parallel with growth of the 3.4 μm complex due to addition of chemical groups. In comparison with ISO data for Orion Bar D2 and H2S1, the outer part of the Red Rectangle nebula has a 3.28 $\mu\text{m}/3.30 \mu\text{m}$ ratio comparable to that of Orion Bar D2, but H2S1, which is nearer the ionisation front, has 3.28 μm and 3.30 μm components that are approximately equal in strength.

This pattern appears to follow the level of extinction, A_V , having values of about 4.2 (Red Rectangle on-star though strongly dependent on geometry due to the disk (Men’shchikov et al. 2002; Vijn, Witt & Gordon 2005a)),

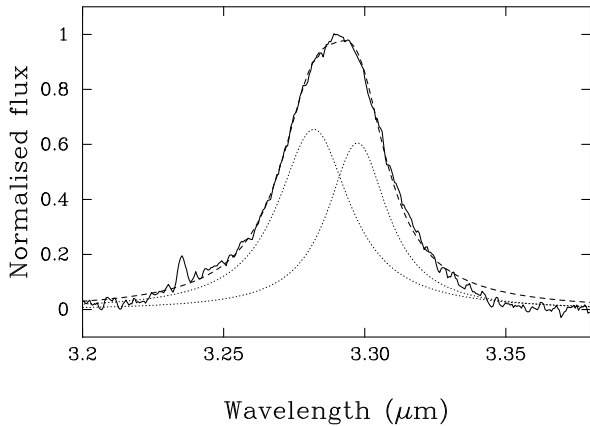


Figure 11. Two-component Lorentzian fit to the 3.3 μm profile towards Orion Bar H2S1 as recorded by ISO SWS.

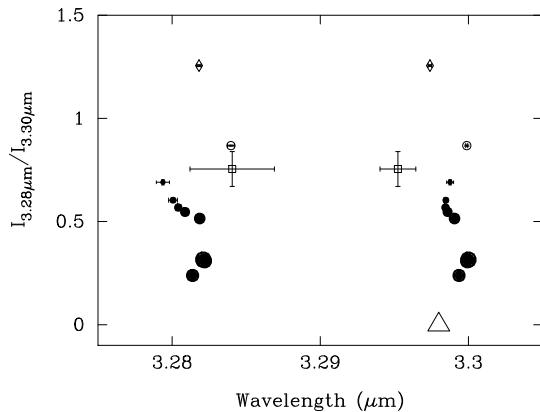


Figure 12. Plot of 3.28 μm /3.30 μm intensity ratio *vs.* peak wavelength of the fitted two-component Lorentzian profiles. The symbols are: \diamond — Orion Bar HS21, \square — Orion Bar D2, \circ — Red Rectangle (ISO data), and \bullet — Red Rectangle (this work) where the diameter of the circle (\bullet) is inversely proportional to the offset from the star and the data extend in this figure to $6''.3$. The open \triangle indicates the on-star datum for which the 3.28 μm feature is absent.

$A_V > 4$ for Orion D2 (Tielens et al. 1993) and $A_V < 4$ for Orion H2S1 (Tielens et al. 1993). This implies that only in regions of relatively high extinction can smaller PAHs survive as discussed by Vijh, Witt & Gordon (2005b). This does not exclude the possibility of some larger PAHs also near HD 44179 because the observability of IR emission depends also on the intrinsic efficiency of conversion of UV to IR radiation which may well be greater for small PAHs. We also remark that the evolution of material from ‘fresh’ near to HD 44179 to ‘processed’ seems to follow the development of the 3.28 μm feature.

7 SUMMARY AND CONCLUSIONS

A re-analysis of long-slit spectra using a two-component fitting supports the earlier suggestion of two components of the 3.3 μm band in the Red Rectangle nebula, centred near 3.30 μm and 3.28 μm . Both components exhibit small shifts with offset attributable to a temperature decrease. On the basis of band shifts, band ratios and comparison with laboratory data, the observations are consistent with the smallest neutral PAHs in the Red Rectangle being present ‘on’-star (with no 3.28 μm component), with the size of PAHs growing with offset and giving rise the 3.28 μm band.

ACKNOWLEDGMENTS

We thank the UK Panel for the Allocation of Telescope Time for the award of observing time on UKIRT, the National Institute for International Education Department (NIIED) of the Korean Government and The University of Nottingham for a studentship to In-Ok Song. We are grateful to Els Peeters for making available to us the ISO SWS 3.3 μm data in electronic form.

REFERENCES

- Allamandola, L.J., Tielens, A.G.G.M., Barker, J. R., 1989, ApJS, 71, 733
 Bauschlicher, C.W., 2002, ApJ, 564, 782
 Bregman, J.D., Rank, D., Temi, P., Hudgins, D., Kay, L., 1993a, ApJ, 411, 794
 Bregman, J., Rank, D., Sandford, S.A., Temi, P., 1993b, ApJ, 410, 668
 Bregman, J., Larson, K., Rank, D., Temi, P., 1994, ApJ, 423, 326.
 Bujarrabal, V., Castro-Carrizo, A., Alcolea, J., Neri, R., 2005, A&A, 441, 1031 and references therein.
 Cernicharo, J., Heras, A.M., Tielens, A.G.G.M., Pardo, J.R., Herpin, F., Guélin, M., Waters, L.B.F.M., 2001, ApJ, 546, L123
 Chiar J.E., Tielens, A.G.G.M., Whittet, D.C.B., Schutte, W.A., Boogert, A.C.A., Lutz, D., van Dishoeck, E.F., Bernstein, M.P., 2000, ApJ, 537, 749
 Cohen M. et al., 1975, ApJ, 196, 179
 Cohen M., Van Winckel, H., Bond, H.E., Gull, T.R., 2004, AJ, 127, 2362
 de Graauw, T., et al., 1996, A&A, 315, L49
 Geers, V.C., Augereau, J., Pontoppidan, K.M., Käuff, H., Lagrange, A., Chauvin, G., van Dishoeck, E.F., 2005, High resolution infrared spectroscopy in astronomy, ed. H. U. Käuff, R. Siebenmorgen, and A.F.M. Moorwood. ESO astrophysics symposia (Berlin: Springer), 239
 Geballe, T.R., Tielens, A.G.G.M., Allamandola, L.J., Moorhouse, A., Brand, P.W.J.L., 1989, ApJ, 341, 278
 Hony, S., Van Kerckhoven, C., Peeters, E., Tielens, A.G.G.M., Hudgins, D.M., Allamandola, L.J., 2001, A&A, 370, 1030
 Hora, J.L., Deutsch, L.K., Hoffmann, W.F., Fazio, G.G., 1996, AJ, 112, 2064
 Joblin, C., Boissel, P., Léger, A., D’Hendecourt, L., Défourneau, D., 1995, A&A, 299, 835

- Kerr T.H., Hurst M.E., Miles J.R., Sarre P.J., 1999, MNRAS, 303, 446
- Mékarnia, D., Rouan, D., Tessier, E., Dougados, C., Lefèvre, J., 1998, A&A, 336, 648
- Men'shchikov, A.B., Balega, Y.Y., Osterbart, G., Weigelt, G., 1998, New Astron., 3, 601
- Men'shchikov, A.B., Schertl, D., Tuthill, P.G., Weigelt, G., Yungelson, L.R., 2002, A&A, 393, 867
- Miyata, T., Kataza, H., Okamoto, Y. K., Onaka, T., Sako, S., Honda, M., Yamashita, T., Murakawa, K., 2004, A&A, 415, 179
- Murakawa, K., Tamura, M., Suto, H., Miyata, T., Gledhill, T.M., Hough, J.H. 2003, Proc. SPIE, 4843, 196
- Osterbart, R., Langer, N., Weigelt, G., 1997, A&A, 325, 609
- Pauzat, F., Ellinger, Y., 2001, MNRAS, 324, 355 and references therein.
- Peeters, E., Hony, S., Van Kerckhoven, C., Tielens, A.G.G.M., Allamandola, L.J., Hudgins, D.M., Bauschlicher, C.W., 2002a, A&A, 390, 1089
- Peeters, E. et al., 2002b, A&A, 381, 571
- Roddier, F., Roddier, C., Graves, J. E., Northcott, M. J., 1995, ApJ, 443, 249.
- Schutte, W.A., Tielens, A.G.G.M., Allamandola, L.J., 1993, ApJ, 415, 397
- Sellgren, K., Tokunaga, A.T., Nakada, Y., 1990, ApJ, 349, 120
- Sellgren, K., 2001, Spectrochim. Acta A, 57, 627
- Sloan, G.C., Bregman, J.D., Geballe, T.R., Allamandola, L.J., Woodward, C.E., 1997, ApJ, 474, 735
- Song, I.-O., Kerr, T.H., McCombie, J., Sarre, P.J., 2003, MNRAS, 346, L1
- Tielens, A.G.G.M., Meixner, M.M., van der Werf, P.P., Bregman, J., Tauber, J.A., Stutzki, J., & Rank, D., 1993, Science, 262, 86
- Tielens, A.G.G.M., Hony, S., Van Kerckhoven, C., Peeters, E., 1999, in Proc. ESA Symp., The Universe as seen by *ISO*, ed. P. Cox & M.F. Kessler, (ESA SP-427; Noordwijk: ESA), 579
- Tokunaga, A.T., 1997, in ASP Conf. Ser. 124, Diffuse Infrared Radiation and the IRTS, ed. H. Okuda, T. Matsumoto, T. Roellig (San Francisco: ASP), 149
- Tokunaga, A.T., Sellgren, K., Smith, R.G., Nagata, T., Sakata, A., Nakada, Y., 1991, ApJ, 380, 452
- Tuthill, P.G., Men'shchikov, A.B., Schertl, D., Monnier, J.D., Danchi, W.C., Weigelt, G., 2002, A&A, 389, 889
- van Diedenhoven, B., Peeters, E., Van Kerckhoven, C., Hony, S., Hudgins, D.M., Allamandola, L.J., Tielens, A.G.G.M., 2004, ApJ, 611, 928 and references therein.
- Van Kerckhoven, C. et al., 2000, A&A, 357, 1013
- Vijh, U.P., Witt, A.N., Gordon, K.D., 2004, ApJ, 606, L65
- Vijh, U.P., Witt, A.N., Gordon, K.D., 2005a, ApJ, 619, 368
- Vijh, U.P., Witt, A.N., Gordon, K.D., 2005b, ApJ, 633, 262
- Waelkens C., Van Winckel H., Waters L.B.F.M., Bakker E.J., 1996, A&A, 314, L17
- Wagner, D.R., Kim, H.-S., Saykally, R.J., 2000, ApJ, 545, 854
- Waters L.B.F.M. et al., 1998, Nature, 391, 868